

Genetic selection designed to stabilize proteins uncovers a chaperone called Spy

Shu Quan^{1,2}, Philipp Koldewey^{1,2}, Tim Tapley^{1,2}, Nadine Kirsch^{1,2}, Karen M. Ruane³, Jennifer Pfizenmaier^{1,2}, Rong Shi³, Stephan Hofmann^{1,2}, Linda Foit^{1,2}, Guoping Ren^{1,2}, Ursula Jakob², Zhaohui Xu^{4,5}, Miroslaw Cygler^{3,6}, and James C. A. Bardwell^{1,2}

¹Howard Hughes Medical Institute

²Department of Molecular, Cellular and Developmental Biology, University of Michigan, Ann Arbor, Michigan, USA

³Department of Biochemistry, McGill University, Montreal, Quebec, Canada

⁴Department of Biological Chemistry, University of Michigan, Ann Arbor, Michigan, USA

⁵Life Sciences Institute, University of Michigan, Ann Arbor, Michigan, USA

⁶Biotechnology Research Institute, NRC, Montreal, Quebec, Canada

Abstract

To optimize the *in vivo* folding of proteins, we linked protein stability to antibiotic resistance, thereby forcing bacteria to effectively fold and stabilize proteins. When we challenged *Escherichia coli* to stabilize a very unstable periplasmic protein, it massively overproduced a periplasmic protein called Spy, which increases the steady-state levels of a set of unstable protein mutants up to 700-fold. *In vitro* studies demonstrate that the Spy protein is an effective ATP-independent chaperone that suppresses protein aggregation and aids protein refolding. Our strategy opens up new routes for chaperone discovery and the custom tailoring of the *in vivo* folding environment. Spy forms thin, apparently flexible cradle-shaped dimers. Spy is unlike the structure of any previously solved chaperone, making it the prototypical member of a new class of small chaperones that facilitate protein refolding in the absence of energy cofactors.

The folding of many proteins is assisted by molecular chaperones and other folding helpers in the cell. Many chaperones act by inhibiting off-pathway events, such as aggregation, and serve a broad range of substrates in a stoichiometric manner. *In vitro* assays for chaperone activity are thus almost by necessity relatively insensitive, making these assays more useful

Users may view, print, copy, download and text and data- mine the content in such documents, for the purposes of academic research, subject always to the full Conditions of use: http://www.nature.com/authors/editorial_policies/license.html#terms

Correspondence should be addressed to J.C.A.B. (jbardwel@umich.edu).

Accession Code: The coordinates and structure factors have been deposited in the Protein Databank with accession code 3O39.

Author Contributions: J.C.A.B. designed the study and wrote the manuscript with contributions from M.C and S.Q.. S.Q., P.K., T.T., N.K., K.R., R.S., J.P., S.H. and G.R. performed the experiments and collected and analyzed the data. J.C.A.B., X.U. and M.C. further analyzed the data. L.F. and U.J. provided technical support and conceptual advice.

Competing Financial Interests: The authors declare no competing financial interests.

Note: Supplementary Information is available on the Nature Structural & Molecular Biology website.

in studying previously identified chaperones than in identifying new ones in crude cell lysates. Instead of being discovered directly for their capacity to assist *in vivo* protein folding processes, many chaperones were initially characterized because of their induction by stress conditions². The lack of a sensitive and general *in vivo* assay for chaperone activity led us to wonder how complete the list of known chaperones is.

Previously, we developed a genetic system that directly links increased protein stability to increased antibiotic resistance³ and thereby provides a selectable and quantitative *in vivo* measure of protein stability³. Our selection system makes use of a sandwich fusion between β -lactamase and unstable proteins, which effectively links the stability of the inserted proteins to the penicillin resistance of the host strain. We showed that β -lactamase tolerates the insertion of a well-folded protein in a surface loop (at position 197) and still retains enzymatic activity (Fig. 1). However, insertion of unstable proteins at this site negatively affects β -lactamase activity and decreases penicillin V resistance (Pen^V^R) *in vivo*³. This strategy allowed us to select for stabilized protein variants of a well characterized protein, immunity protein 7 (Im7)³.

Now, we hypothesized that a similar strategy could even be used to select for host variants that alter the *in vivo* folding environment of individual proteins by enhancing protein folding or stability, either specifically or generally. Because our system functions in the periplasm, it may also provide an opportunity to explore protein folding in what has generally been considered to be a relatively chaperone-poor environment and, in doing so, uncover new chaperones. In selecting for host variants that stabilized a very unstable Im7 mutant, we discovered variants that massively overproduce a previously poorly characterized protein called Spy. We found Spy to be the founding member of a new class of chaperones that have a novel cradle-shaped structure and function as ATP-independent folding chaperones in the periplasm of *Escherichia coli*.

Results

Selection for optimized protein folding *in vivo*

We designed a dual selection system by inserting the same unstable test protein Im7-L53A I54A into the middle of β -lactamase, which encodes Pen^V^R, and DsbA which encodes cadmium resistance (CdCl₂^R)⁴, as sandwich fusions (Fig. 1). Our overall experimental scheme is illustrated in Fig. 2. The two resistance markers operate via very different mechanisms^{4, 5} and thus provide an independent measure of the stability of the inserted protein. In strains that co-express both fusions, we reasoned that host mutations that simultaneously increased Pen^V^R and CdCl₂^R should positively affect the one thing that these two constructs apparently have in common, namely the stability of the inserted protein. Insertion of Im7 variants into DsbA after residue Thr99, a site that can tolerate protein insertions (Fig. 1 and Supplementary Fig. 1), revealed an excellent correlation between CdCl₂^R and Im7 variant stability (Fig. 1c). CdCl₂^R also correlated well with Pen^V^R when the same Im7 variants were inserted into β -lactamase (Fig. 1d). The highest resistance to both antimicrobials came from the most stable Im7 variants. These results suggested that host variants that stabilize Im7 should increase both Pen^V^R and CdCl₂^R and thus should be easily selected for on this basis.

We searched for host mutations that enable the proper folding of Im7-L53A I54A, a very unstable Im7 variant⁶. Using ethyl methanesulfonate (EMS), we randomly mutagenized strain SQ1306, which contains sandwich fusions between this unstable Im7 variant and both DsbA and β -lactamase. We selected for variants with enhanced PenV^R and then screened those for enhanced CdCl₂^R.

Plate screens revealed that about 13% (35 of 263) of the strains that had gained PenV^R had simultaneously acquired resistance to CdCl₂. Ten independently isolated mutant strains that were resistant to both PenV and CdCl₂ (EMS1–EMS10, Supplementary Table 1a) were selected for further analysis. Eight of these contained substantially elevated levels of the β -lactamase-Im7 fusion protein, as determined by quantitative Western blots (Supplementary Fig. 2). Since EMS4 and EMS9 contained the highest amounts of the sandwich fusion protein and exhibited resistance to high concentrations of both PenV and cadmium they were chosen for further analysis. To confirm these host variants had improved the folding and consequently increased the protein levels of the Im7 protein itself, we transformed EMS4 and EMS9 with plasmids encoding Im7 and three different destabilized Im7 mutants in the absence of the fusion. Both EMS4 and EMS9 strain backgrounds accumulated large amounts of Im7 proteins in the periplasm, in contrast to the parental PenV^S/CdCl₂^S strain SQ1306 (Fig 3a). Quantification using an Agilent bioanalyzer showed that Im7 proteins made up 7-10% of the periplasmic content in EMS4 and EMS9, a 34- to 92-fold increase over the wild-type strain (Fig. 3a, Tables 1 and Supplementary Table 1b). The Im7 proteins were extracted from the periplasm in the absence of detergent, indicating that they accumulate in a soluble form.

Variants massively overexpress the periplasmic protein Spy

In examining the periplasmic extracts of the Im7 overexpressing strains, it was impossible to ignore the strong induction of a 15.9 kD protein, which was identified by mass spectrometry analysis as Spy (Spheroplast protein Y)⁷. The Spy protein accounted for up to 48% of total periplasmic content in eight of the ten tested PenV^R/CdCl₂^R EMS mutant strains (Fig. 3, Supplementary Fig. 2 and Supplementary Table 1b), suggesting that Spy overexpression might be involved in the stabilization of our Im7 variants.

Spy expression is under the control of the Bae and Cpx periplasmic stress response systems⁷⁻⁹, which are induced by a variety of stress conditions known to cause protein unfolding and aggregation^{2, 10}. To identify the mutation(s) that caused the massive up-regulation of Spy expression in EMS4 and EMS9, we sequenced the *spy* gene, its regulators *cpxARP* and *baeRS*, and a number of other candidate genes, picked because they encode periplasmic chaperones, proteases, stress response regulators or multidrug exporters, *surA*, *skp*, *fkpA*, *prc*, *degP*, *ptr*, *ompP*, *ompT*, *rcsABCDF* and *mdtABCD* and their upstream regulator sequences. We discovered that both EMS4 and EMS9 contained mutations in *baeS* but not in any of the other sequenced genes or regulatory sequences (Supplementary Table 1c). We then sequenced the *baeS* gene in all other independently isolated PenV^R/CdCl₂^R strains (EMS1–EMS10) and determined that it was mutated in all strains except EMS7, a strain that failed to overproduce Spy or Im7. A total of six different mutations were found in *baeS* (Supplementary Table 1c).

BaeS is a putative histidine kinase that together with the proposed response regulator BaeR makes up the two-component BaeSR envelope stress response regulation system^{2, 7-9}; this system has previously been shown to regulate *spy* and a few other periplasmic stress genes. We picked one *baeS* mutation, *baeS-R416C*, for further analysis. We established that the *baeS-R416C* mutation was necessary and sufficient for enhanced Im7 expression (Supplementary Fig. 3). Transcriptional analysis of EMS4 revealed not only a massive up-regulation of *spy* mRNA but also a significant induction of other known downstream targets of BaeSR (Supplementary Table 1d), suggesting that the *baeS-R416C* mutation caused the constitutive activation of the BaeSR envelope stress response.

Spy overexpression is sufficient to enhance Im7 expression

To determine if Spy overproduction alone is responsible for the enhanced levels of the unstable Im7 protein, or whether other BaeSR-regulated proteins are involved as well, we overproduced Spy from the pTrc promoter to levels similar to those seen in the EMS4 mutant, in a *baeSR* null background. We found that for the various destabilized Im7 mutants, overexpression of Spy, even in the absence of a functional BaeSR system, led to soluble Im7 levels that were very similar to those observed in EMS4 by SDS-PAGE analysis (Fig. 3b). Quantification of Im7 and Spy levels showed that upon Spy overexpression, Im7 levels increased 100- to 700-fold (Table 1). The overexpression of downstream targets of BaeSR other than *spy* apparently does not contribute to the observed PenV resistant phenotype, as their individual deletions had no effect on PenV resistance (Supplementary Fig. 3). Based on these results, we concluded that Spy overproduction is necessary and sufficient to increase the levels of soluble periplasmic Im7. Strains deficient in the protease DegP exhibited increased levels of Im7 (Supplementary Fig. 4a), so it appears that Spy is acting at least in part to protect Im7 from proteolysis.

Spy has chaperone activity *in vitro*

Although sequences homologous to Spy are present in a wide variety of enterobacteria, protobacteria and some cyanobacteria (Supplementary Fig. 5), very little was previously known about Spy function⁷. Deletion of *spy* was reported to cause slight induction of *degP* and *rpoH*, two genes under the control of *rpoE*, a stress response system involved in outer membrane protein biogenesis leading to the suggestion that Spy may also be involved in this process¹¹. Using quantitative reverse transcription polymerase chain reaction (qRT-PCR), we were unable to detect significant induction of these or other periplasmic stress regulated genes upon deletion of *spy* in our strain background (Supplementary Table 1d), suggesting that *spy* deletion does not cause significant defects in membrane integrity.

Our finding that Spy overexpression leads to the accumulation of an otherwise highly unstable protein instead suggested that Spy might function as a chaperone that facilitates protein folding in the bacterial periplasm. To assess its chaperone activity, we purified Spy and analyzed its influence on the aggregation of a number of substrate proteins *in vitro* (Fig. 4a). We first tested the effect of Spy on the aggregation of thermally denatured malate dehydrogenase (MDH) and found that addition of increasing amounts of Spy significantly reduced protein aggregation. Even sub-stoichiometric quantities of Spy effectively inhibited the aggregation process, suggesting that Spy is a highly efficient chaperone. Analysis of the

effects of Spy on urea-denatured MDH revealed similar results and showed that Spy effectively prevents MDH from aggregating. We found that Spy, which is strongly induced by the protein denaturant ethanol⁹, protects MDH from ethanol-mediated aggregation. We also observed a strong suppression of aggregation of chemically denatured aldolase and glyceraldehyde-3-phosphate dehydrogenase (GAPDH) by Spy. Given that heat, urea and ethanol use different mechanisms to unfold proteins, we concluded that Spy must have a general affinity for a wide range of different protein unfolding intermediates. Combined, our results strongly suggested that we identified a new, general chaperone in the periplasm of *E. coli*.

Most known ATP-dependent chaperones, such as the DnaK and GroEL systems, function as folding chaperones¹². They use cycles of ATP binding and hydrolysis to regulate substrate binding and release, thus facilitating protein folding¹². In contrast, most known ATP-independent chaperones function as holding chaperones, which prevent protein aggregation but usually lack the ability to support protein folding¹³. To test if Spy can support protein folding, even though it is localized to the ATP-devoid environment of the bacterial periplasm, we analyzed its influence on the refolding yield of chemically and thermally unfolded proteins. We found that Spy significantly increased the refolding yield of a number of substrates (Fig. 4b). Because the assays were performed in the absence of any cofactors, these results strongly suggest that Spy has intrinsic protein folding capacity, providing an excellent explanation of how Spy overexpression is sufficient to substantially increase the amount of folded Im7 protein *in vivo*.

Spy protects proteins from tannin inactivation

qRT-PCR-based measurements indicated that *spy* mRNA is induced nearly 500-fold in response to tannin treatment¹⁴. The gene for IbpB, an *E. coli* small heat shock protein homolog also involved in inhibiting protein aggregation, is induced 48-fold by tannins, making it second only to *spy* in induction by tannins¹⁴. Tannins, which have long been used to tan leather, are the fourth most abundant component of vascular plant tissue and are synthesized by plants as a protection against bacterial and fungal infections¹⁵. Tannins are thought to be responsible for the astringent taste of many human food substances including cheap red wine, strong tea, and unripe fruit¹⁶. Some forage crops contain up to 25% tannins by dry weight. *E. coli* found in the gut of herbivores is thus exposed to high concentrations of tannins, driving it to develop tannin resistance¹⁷. Tannins can have human disease-related antimicrobial effects¹⁸. The tannins present in cranberry juice, for instance, act as potent inhibitors of the attachment of pathogenic *E. coli* to the uroepithelium and are thought to explain the effectiveness of cranberry juice in preventing urinary tract infections¹⁹. Only small quantities of tannins are required to aggregate proteins, a feature that may be responsible for their antimicrobial activity²⁰. Their astringent taste in foods may be due to the precipitation of mouth proteins²¹. The astringent taste of strong tea is often reduced by addition of milk, which drives co-precipitation of the tannins with the disordered protein casein that is present in milk²¹. Tannic acid has also been reported to have potent anti-amyloidogenic activity²²⁻²⁴.

We tested the effects of Spy on tannin-mediated inactivation of the *E. coli* membrane protein DsbB (Fig. 5a), aldolase (Fig. 5b) and the *E. coli* periplasmic protein alkaline phosphatase (Fig. 5c). Spy protected all three proteins from tannic acid-induced activity loss. Consistent with this *in vitro* result, we discovered that *spy* null mutants are highly sensitive to tannins (Fig. 5d) and show decreased alkaline phosphatase activity *in vivo* (Supplementary Fig. 2). *baeSR* mutants have been reported to be tannin sensitive¹⁴, and we found that most, but not all, of the tannin sensitivity could be attributed to induction of Spy (Fig. 5d). The antimicrobial action of tannins can substantially alter the microbial content of the gut; indeed, the relatively high tannin resistance of enterobacteria, which we show here is mediated at least in part by Spy, appears to be responsible for allowing the population of fecal enterobacteria to increase up to 19-fold in rats fed a high tannin diet¹⁷. We conclude that the induction of Spy is likely to be involved in protecting cells from tannin-induced protein aggregation and inactivation *in vitro* and *in vivo*.

Spy may not have a regulatory role like its homolog CpxP

The Spy protein is 29% identical to CpxP, an inhibitory component of the CpxRA regulatory system²⁵. CpxP binds to the periplasmic domain of CpxA, inhibiting its autokinase activity. The presence of unfolded proteins causes the release of CpxP, thereby activating the Cpx response^{25, 26}. These observations suggested that CpxP might be acting as one of the very few known periplasmic chaperones, targeting itself and its unfolded protein cargo to the protease DegP for degradation^{27, 28}. We found that CpxP has weak chaperone activity *in vitro* and CpxP overproduction causes the accumulation of Im7 in otherwise wild-type strains (Supplementary Fig. 4). To assess whether Spy might be involved in regulating BaeSR or the other periplasmic stress response systems, we carried out qRT-PCR in strains either lacking or overexpressing *spy* (Supplementary Table 1d). We found no notable influence on the expression of *baeS*, *cpx*, *rpoE*, *rpoH*, *rcs* or *psp* regulated genes, suggesting that Spy, unlike CpxP, may not be playing a major regulatory role. Instead, our results strongly suggest that Spy functions directly as a molecular chaperone.

Spy has a novel chaperone fold—an α -helical cradle

To gain insights into the mechanism of Spy's chaperone action, we crystallized and determined the three-dimensional structure of His-tagged Spy (Table 2). The crystal structure shows that Spy molecules associate into tightly bound dimers. Size exclusion chromatography and analytical ultracentrifugation (Supplementary Fig. 6) confirmed this oligomerization state and revealed that Spy is also dimeric in solution. Each Spy monomer consists of four α -helices (α 1– α 4). The 28 N-terminal residues and 14 C-terminal residues are disordered in the crystal. Helices α 1, α 2 and α 3 fold into a hairpin, with α 1 and α 2 forming one arm and α 3 the other arm (Fig. 6a and Supplementary Fig. 6). Helix α 3 has nine turns and is bent in the middle by $\sim 30^\circ$ due to partial unwinding at Met85–Glu86. The N-terminal half of α 3 is parallel to α 2, whereas its C-terminal half is parallel to α 1. Helix α 4 runs antiparallel to α 3 and is inclined to it by $\sim 45^\circ$. The first six ordered N-terminal residues, Phe29–Leu34, assume an extended conformation and follow along helix α 4. Following the submission of our work, the crystal structure of Spy was determined as part of a high-throughput effort²⁹; as expected, this structure is very similar to ours. The Spy dimer is formed through the antiparallel coiled-coiled interaction. The shape of the dimer is rather

unusual, with one surface highly concave and the other convex, reminiscent of a cradle. The bottom of this cradle is formed by helices $\alpha 3$, the sides by the connection between helices $\alpha 1$ and $\alpha 2$ and the tips by helices $\alpha 1$ and $\alpha 4$. The cradle is extremely thin in cross section; its average thickness is 9.2 Å (Supplementary Fig. 6). The contacts between the two monomers are extensive, burying a surface of ~ 1850 Å² per monomer upon dimerization and suggesting high dimeric stability. Although the concave surface has an overall positive charge²⁹, it is also lined with a number conserved apolar side chains, localized in two clusters that are exposed as hydrophobic patches (Fig. 6b,c).

Substrate interaction with Spy

To investigate the interaction between Spy and protein substrates, we labeled Spy with two different environmentally sensitive probes, acrylodan and 4-(N-(iodoacetoxy)ethyl-N-methyl)amino-7-nitrobenz-2-oxa-1,3-diazole (IANBD). Probe attachment sites were made by substituting cysteines at six different positions; these included residues exposed to both the concave (R89C, H96C) and convex sides of the cradle (E59C, K77C), as well as residues within the structurally disordered N and C termini (H24C and A128C) (Fig. 6b). We then determined the influence of substrate addition on the fluorescence of the probe-labeled Spy variants. Changes in the microenvironment near the probes caused by substrate addition could reflect either direct binding to the labeled region of the probe or structural rearrangements within Spy caused by substrate binding.

The Spy variants retained substantial ability to inhibit the aggregation of aldolase, showing that they are at least partially active (Supplementary Table 1e and Supplementary Fig. 7a). For the interaction experiments we used casein as a Spy substrate because unlike most of our other Spy substrates it is intrinsically disordered but soluble; Im7-L53A I54A was also chosen because it is an excellent Spy substrate *in vivo*. Im7-L53A I54A *in vitro* is trapped as a partially unfolded but soluble intermediate³. Analytical gel filtration revealed the presence of an apparently stable complex between Spy and casein (Fig. 7a). As shown in Fig. 7b,c, equimolar addition of casein or Im7 significantly decreased Spy-mediated refolding of MDH. We interpreted these data as likely due to direct competition for the same binding site on Spy. We then measured changes in the fluorescence emission spectra of the various labeled Spy variants upon addition of equimolar quantities of casein or Im7-L53A I54A, thereby monitoring potential environmental changes in the vicinity of the labeled residues upon substrate binding. As shown in Fig. 7d and Supplementary Fig. 7b, the fluorescence of acrylodan attached via H24C, E59C, R89C, H96C and A128C significantly increased and blue-shifted with casein addition, suggesting that the region near these residues becomes more hydrophobic in the presence of casein. Acrylodan-labeled H24C and A128C Spy variants also showed fluorescence increases and slight blue shifts upon Im7-L53A I54A addition (Fig. 7e and Supplementary Fig. 7c). IANBD is generally not as sensitive as acrylodan in its ability to reflect changes in the fluorophore environment. Nevertheless, IANBD-labeled H24C, H96C and A128C Spy variants exhibited significantly decreased fluorescence upon casein binding (Supplementary Fig. 7d). Because the fluorescence of IANBD is quenched in hydrophobic environments³⁰, these results suggest that these residues become more hydrophobic in character with casein binding. In contrast, the fluorescence of acrylodan attached via K77C is decreased with casein addition (Fig. 7d),

indicating that the region near this residue probably becomes more hydrophilic with substrate binding. That nearly all our Spy mutants exhibit significant changes in their environment upon substrate addition suggests that substrate binding occurs over large regions of Spy (including both the concave and convex sides of the cradle). Alternatively, major structural rearrangements or higher-order oligomerization reactions could occur within Spy upon substrate binding or both.

Discussion

It may seem surprising that a chaperone as effective as Spy has remained unstudied in an organism as well characterized as *E. coli*. However, because chaperones are usually effective only in stoichiometric quantities, chaperone assays are generally not sensitive enough to enable their purification from crude lysates by activity. Instead, chaperones have often been first identified because their genes are induced in protein unfolding conditions². Our approach of linking folding to selectable markers opens up the possibility of directing evolution to alter the *in vivo* folding environment to specifically enhance the folding of a given unstable protein and provides a new route for chaperone discovery.

Spy has a unique cradle shape that is unlike any other chaperone whose structure is known. Spy lacks a significant globular core and would therefore be expected to display higher flexibility than the average globular protein. The molecule averages 9.2 Å in thickness, less than the 12Å diameter of a single α -helix. Its thinness places a disproportionate number of side chains on the protein surface. The highest backbone temperature factors are observed in surfaces and bumps extending from the concave side of the cradle, particularly in the connectors between helices α_1 and α_2 , which form the sides of the cradle, suggesting the possibility for bending and twisting of the molecule (Fig. 6d). Spy's shape combined with its apparent flexibility leads us to propose a model for Spy action that involves the shielding of aggregation-sensitive regions on substrate proteins, which are revealed upon partial unfolding by interaction with Spy. Spy's apparently highly flexible nature may allow the chaperone to accommodate a variety of partially unfolded protein substrates. The extremely high flexibility of another periplasmic chaperone HdeA, for instance, appears to allow it to bind numerous substrate proteins and prevent aggregation³¹.

Addition of 4 mM tannic acid results in the massive induction of Spy so that it comprises ~25% of periplasmic proteins (Supplementary Fig. 2d), similar to the induction seen in our *baeS* constitutive EMS strains (Supplementary Table 1b). Of *E. coli*'s ~4280 genes, *spy* is one of those most strongly induced by butanol^{32, 33}, a protein unfolding agent³⁴, leading to Spy comprising ~20% of periplasmic proteins (Supplementary Fig. 2d). Ethanol, another well known protein denaturant and potent inducer of the heat shock response³⁵, also strongly induces Spy so that it makes up ~5% of periplasmic proteins⁹ (Supplementary Fig. 2d). Spy is also strongly induced by other conditions that induce protein unfolding, such as overproduction of miss-folded PapG and NlpE⁷. Thus, strong induction of Spy is physiological, not something that only occurs in our BaeS constitutive mutants. That Spy is induced so strongly by protein unfolding or precipitation agents that it becomes up to 25% of the periplasmic contents implies a pressing need for it to respond to unfolding conditions. Other chaperones also attain high percentages after stresses that unfold proteins. GroEL, for

instance, becomes 12% of the total cellular protein during growth at 46 °C³⁶, but the abundance of Spy is more extreme, particularly when calculated on a molar basis. The total concentration of protein in cells is $\sim 300 \text{ g l}^{-1}$ ³⁷, allowing one to calculate the molar concentration of the 31 kDa Spy dimer in the periplasm to be up to 2.4 mM. GroEL functions as a 790 kDa 14-mer, so its molar concentration in the cell when 12% of total cellular contents is only about 0.05 mM or about 50-fold less abundant on a molar basis than the physiological levels of induced Spy. Even though Im7 can attain $\sim 10\%$ of the cell protein upon Im7 overproduction, Spy is even more abundant; upon Spy overproduction, approximately two Spy dimers are present in the periplasm for every Im7 monomer.

The extreme abundance of Spy leads us to propose a speculative model for Spy action in which it protects proteins *in vivo* by binding to aggregation prone regions exposed on the surface of unstable proteins, coating these regions (or possibly even the entire unstable protein) with a thin layer that inhibits proteolysis and/or aggregation. Upon Spy overproduction, the levels of unstable Im7 mutants go from barely detectable to up to 10% of periplasmic extracts (Supplementary Table 1d), likely because Spy is very effective in inhibiting *in vivo* proteolysis and/or aggregation. Changes in the fluorescence of environmentally sensitive probes labeled with acrylodan or IANBD are consistent with either Spy binding to substrates via large parts of the molecule or major rearrangements occurring in the Spy structure upon substrate binding or both. Defining the precise substrate binding site, the stoichiometry of its interaction with substrates, and its precise mechanism of action, including the possible involvement of co-chaperones, awaits future experimentation.

Although suppression of protein aggregation does not require energy, release and refolding of bound substrate proteins usually does³⁸. ATP is absent in the periplasm and in our assays was not required for the refolding function of Spy, indicating that the chaperone activity of Spy is ATP-independent. Thus, Spy appears to be one of the very few chaperones that actively support protein refolding in the absence of any obvious energy source, suggesting that Spy uses a mechanism to control substrate binding and release that is different from that of previously characterized chaperones. How Spy enables refolding in the absence of energy cofactors is a provocative question for future research. At this point, we can only speculate that the apparently highly dynamic nature of the Spy structure may permit structural fluctuations that not only allow it to mold to various proteins but also enable it to release them.

Methods

Mutagenesis and selection to identify new periplasmic folding factors

Bacteria containing the plasmids pBR322bla: :GS linker Im7 L53A I54A and pBAD33dsbA: :GS linker Im7 L53A I54A, which encode sandwich fusions of Im7 L53A I54A with β -lactamase and *dsbA* respectively, were subject to EMS mutagenesis³⁹, and mutants resistant to $1500 \mu\text{g ml}^{-1}$ penicillin and 0.5 mM CdCl_2 were selected. Western blotting of total cell extracts was used to detect the levels of β -lactamase-Im7 fusion protein present in these mutant strains. Following transformation with plasmids that encode wild-type Im7 and various destabilized Im7 mutants expressed under the pTrc promoter,

periplasmic extracts were prepared as previously described⁴⁰, and the pattern of soluble periplasmic protein expression was examined on SDS gels (Invitrogen). The level of Im7 and Spy present in these extracts was quantified using a Bioanalyzer 2100 (Agilent) as described below.

Quantification of proteins

The amount of the sandwich fusion protein β -lactamase-Im7 L53A I54A in SQ1306 and EMS1–EMS10 was quantified by Western blot with anti- β -lactamase antibody using whole cell lysate as described previously³ with minor modifications. To quantify plasmid-encoded Im7 (wild-type and variants) expressed in the absence of the fusion, cells were grown to mid-log phase in LB medium at 37 °C. Im7 protein expression was induced with 2 mM IPTG for 2 h. Addition of IPTG also induces the expression of Spy when the pTrc-spy plasmid is present. Periplasmic extractions were prepared as described previously⁴⁰, and the proteins were separated using a Bioanalyzer 2100 (Agilent) with the high sensitivity protein 250 kit and the conditions specified by the manufacturer. To visualize the tiny signal corresponding to Im7 present in the absence of Spy expression, a pico labeling protocol was applied (Agilent technical note, publication number: 5990-3703EN). Prior to labeling, periplasmic extractions were diluted to different extents to ensure the linear relationship between Im7 amount and signal. Protein ratios were determined by integrating the trough-to-trough peak area. The high sensitivity of the 250 kit and the pico labeling protocol allowed the visualization and quantification of the very small amount of Im7 present in the absence of Spy, an amount that was not detectable on either Coomassie blue-stained SDS-PAGE gels or on the Agilent bioanalyzer using either the 80 or 230 protein kits. Although excellent for determining the ratio of a single defined protein present in different sample preparations, we reasoned that differences in labeling efficiencies between different proteins would make this protocol suboptimal for percentages of the total protein. Instead, the percentage of Spy and Im7 was quantified in overproducing strains using the protein 80 kit (Agilent) without labeling. Areas corresponding to Spy or Im7 peaks were compared to the total area of all proteins present in the periplasmic extract. In the absence of Spy, the Im7 peak was not detectable; therefore, the percentage of Im7 was calculated by dividing the Im7 percentage in the presence of Spy overexpression with the fold increase of Im7 level. For example, Im7 is 10% of total periplasm in SQ1405. Im7 expression increased 34-fold in SQ1405 compared to SQ1413. The percentage of Im7 in SQ1413 was therefore calculated to be 0.3%. The percentage of Spy present in periplasmic extracts in different EMS strains was quantified similarly with the protein 80 kit.

Crystallization

Initial crystallization conditions of the mature form of Spy (residues 1–138) with N-terminal His₆-tag were identified using the AmSO₄ suite (Qiagen Inc., Canada). Spy contains 161 residues of which 23 constitute the signal peptide that directs Spy to the periplasm. Our residue numbers refer to the mature, periplasmic form of Spy, which contains 138 residues; the N-terminal His₆-tag is left un-numbered. The SeMet-substituted protein was crystallized under the same conditions. The best diffracting crystals were obtained by mixing 1 μ l protein in the final buffer with 1 μ l of reservoir solution containing 0.3 M CdCl₂ and 2.4 M

AmSO₄ under the vapor diffusion hanging drop method. Prior to data collection, the crystals were cryoprotected in paratone and flash frozen in liquid nitrogen.

Data collection and processing

The diffraction data were collected from a single crystal at the CMCF-1 beamline at the Canadian Light Source (CLS), Saskatoon, Saskatchewan at the Se absorption edge (wavelength of 0.9792 Å) to 2.6 Å resolution at 100 K. Data were processed and scaled using DENZO and SCALEPACK in the HKL2000 suite⁴¹.

Structure determination and refinement

The structure was solved by the single anomalous diffraction method. Of the 22 expected Se atoms in the asymmetric unit, 8 were located and refined using autoSHARP⁴². These sites were used to obtain preliminary phases. The model was built manually in Coot⁴³ using the Se sites as reference points. Several cycles of refinement using REFMAC⁵⁴⁴ followed by model rebuilding were carried out. The final refinement was performed with PHENIX⁴⁵ and included the TLS model for thermal motions. The His₆ tag and the first 28 residues as well as the last 14 C-terminal residues are disordered. The final model includes the central 96 residues for each monomer. Of these, 11 long side-chains in molecule A and 15 in molecule B were only partially modeled. The pertinent data are shown in Table 2. The model has good geometry as analyzed by Molprobity⁴⁶, 96.9% (309/319) of all residues are in the favored region and 100% of all residues are in the allowed region.

Additional methods

A detailed description of all other methods is given in Supplementary Methods.

Supplementary Material

Refer to Web version on PubMed Central for supplementary material.

Acknowledgments

We thank G. Morgan and S. Radford for communicating results prior to publication, and for the kind gift of Im7-L53A I54A protein, T. Franzmann for performing the ultracentrifugation experiments, D. Reichmann, C. Creemers, and A. Malik for advice, M. Lei and Y. Chen for providing vector and reagents for Spy purification, and C. Munger for initial purification and crystallization of Spy. Protein identification was performed by the Protein Structure Facility at the University of Michigan. Diffraction data were collected at the CMCF-1 beamline at the Canadian Light Source, Saskatoon, Saskatchewan, Canada. We would like to thank S. Labiuk for data collection. The Howard Hughes Medical Institute funded this work. M.C. acknowledges financial support from CIHR grant GSP-48370.

References

1. Kerner MJ, et al. Proteome-wide analysis of chaperonin-dependent protein folding in *Escherichia coli*. *Cell*. 2005; 122:209–220. [PubMed: 16051146]
2. Duguay AR, Silhavy TJ. Quality control in the bacterial periplasm. *Biochim Biophys Acta*. 2004; 1694:121–134. [PubMed: 15546662]
3. Foit L, et al. Optimizing protein stability in vivo. *Mol Cell*. 2009; 36:861–871. [PubMed: 20005848]

4. Stafford SJ, Humphreys DP, Lund PA. Mutations in *dsbA* and *dsbB*, but not *dsbC*, lead to an enhanced sensitivity of *Escherichia coli* to Hg²⁺ and Cd²⁺ FEMS Microbiol Lett. 1999; 174:179–184. [PubMed: 10234837]
5. De Pascale G, Wright GD. Antibiotic resistance by enzyme inactivation: from mechanisms to solutions. *Chembiochem*. 2010; 11:1325–1334. [PubMed: 20564281]
6. Spence GR, Capaldi AP, Radford SE. Trapping the on-pathway folding intermediate of Im7 at equilibrium. *J Mol Biol*. 2004; 341:215–226. [PubMed: 15312774]
7. Raffa RG, Raivio TL. A third envelope stress signal transduction pathway in *Escherichia coli*. *Mol Microbiol*. 2002; 45:1599–1611. [PubMed: 12354228]
8. MacRitchie DM, Buelow DR, Price NL, Raivio TL. Two-component signaling and gram negative envelope stress response systems. *Adv Exp Med Biol*. 2008; 631:80–110. [PubMed: 18792683]
9. Bury-Mone S, et al. Global analysis of extracytoplasmic stress signaling in *Escherichia coli*. *PLoS Genet*. 2009; 5:e1000651. [PubMed: 19763168]
10. Price NL, Raivio TL. Characterization of the Cpx regulon in *Escherichia coli* strain MC4100. *J Bacteriol*. 2009; 191:1798–1815. [PubMed: 19103922]
11. Raivio TL, Laird MW, Joly JC, Silhavy TJ. Tethering of CpxP to the inner membrane prevents spheroplast induction of the cpx envelope stress response. *Mol Microbiol*. 2000; 37:1186–1197. [PubMed: 10972835]
12. Hartl FU, Hayer-Hartl M. Converging concepts of protein folding in vitro and in vivo. *Nat Struct Mol Biol*. 2009; 16:574–581. [PubMed: 19491934]
13. Winter J, Jakob U. Beyond transcription—new mechanisms for the regulation of molecular chaperones. *Crit Rev Biochem Mol Biol*. 2004; 39:297–317. [PubMed: 15763707]
14. Zoetendal EG, Smith AH, Sundset MA, Mackie RI. The BaeSR two-component regulatory system mediates resistance to condensed tannins in *Escherichia coli*. *Appl Environ Microbiol*. 2008; 74:535–539. [PubMed: 18039828]
15. Scalbert A. Antimicrobial Properties of Tannins. *Phytochemistry*. 1991; 30:3875–3883.
16. Hernes PJ, et al. Tannin diagenesis in mangrove leaves from a tropical estuary: A novel molecular approach. *Geochim Cosmochim AC*. 2001; 65:3109–3122.
17. Smith AH, Mackie RI. Effect of condensed tannins on bacterial diversity and metabolic activity in the rat gastrointestinal tract. *Appl Environ Microbiol*. 2004; 70:1104–1115. [PubMed: 14766594]
18. Serrano J, Puupponen-Pimia R, Dauer A, Aura AM, Saura-Calixto F. Tannins: Current knowledge of food sources, intake, bioavailability and biological effects. *Mol Nutr Food Res*. 2009; 53:S310–S329. [PubMed: 19437486]
19. Howell AB, Vorsa N, Marderosian AD, Foo LY. Inhibition of the adherence of P-fimbriated *Escherichia coli* to uroepithelial-cell surfaces by proanthocyanidin extracts from cranberries. *N Engl J Med*. 1998; 339:1085–1086. [PubMed: 9767006]
20. Zanchi D, et al. Tannin-assisted aggregation of natively unfolded proteins. *Europhys Lett*. 2008; 82:58001.
21. Hofmann T, et al. Protein binding and astringent taste of a polymeric procyanidin, 1,2,3,4,6-penta-O-galloyl-beta-D-glucopyranose, castalagin, and grandinin. *J Agr Food Chem*. 2006; 54:9503–9509. [PubMed: 17147439]
22. Ono K, Hasegawa K, Naiki H, Yamada M. Anti-amyloidogenic activity of tannic acid and its activity to destabilize Alzheimer's beta-amyloid fibrils in vitro. *BBA-Mol Basis Dis*. 2004; 1690:193–202.
23. Kim W, et al. A high-throughput screen for compounds that inhibit aggregation of the Alzheimer's peptide. *ACS Chem Biol*. 2006; 1:461–469. [PubMed: 17168524]
24. Lee LL, Ha H, Chang YT, DeLisa MP. Discovery of amyloid-beta aggregation inhibitors using an engineered assay for intracellular protein folding and solubility. *Protein Sci*. 2009; 18:277–286. [PubMed: 19177561]
25. Raivio TL, Popkin DL, Silhavy TJ. The Cpx envelope stress response is controlled by amplification and feedback inhibition. *J Bacteriol*. 1999; 181:5263–5272. [PubMed: 10464196]
26. Danese PN, Silhavy TJ. CpxP, a stress-combative member of the Cpx regulon. *J Bacteriol*. 1998; 180:831–839. [PubMed: 9473036]

27. DiGiuseppe PA, Silhavy TJ. Signal detection and target gene induction by the CpxRA two-component system. *J Bacteriol.* 2003; 185:2432–2440. [PubMed: 12670966]
28. Isaac DD, Pinkner JS, Hultgren SJ, Silhavy TJ. The extracytoplasmic adaptor protein CpxP is degraded with substrate by DegP. *Proc Natl Acad Sci U S A.* 2005; 102:17775–17779. [PubMed: 16303867]
29. Kwon E, Kim DY, Gross CA, Gross JD, Kim KK. The crystal structure *Escherichia coli* Spy. *Protein Sci.* 2010
30. Powl AM, Wright JN, East JM, Lee AG. Identification of the hydrophobic thickness of a membrane protein using fluorescence spectroscopy: Studies with the mechanosensitive channel MscL. *Biochemistry (Mosc).* 2005; 44:5713–5721.
31. Tapley TL, et al. Structural plasticity of an acid-activated chaperone allows promiscuous substrate binding. *Proc Natl Acad Sci U S A.* 2009; 106:5557–5562. [PubMed: 19321422]
32. Brynildsen MP, Liao JC. An integrated network approach identifies the isobutanol response network of *Escherichia coli*. *Mol Syst Biol.* 2009; 5:1–13. article # 277.
33. Rutherford BJ, et al. Functional Genomic Study of Exogenous n-Butanol Stress in *Escherichia coli*. *Appl Environ Microbiol.* 2010; 76:1935–1945. [PubMed: 20118358]
34. Miyawaki O, Tatsuno M. Thermodynamic analysis of alcohol effect on thermal stability of proteins. *J Biosci Bioeng.* Oct 12.2010 epub ahead of print.
35. Neidhardt FC, VanBogelen RA, Vaughn V. The genetics and regulation of heat-shock proteins. *Annu Rev Genet.* 1984; 18:295–329. [PubMed: 6442118]
36. Neidhardt FC, et al. Identity of the B56.5 protein, the A-protein, and the groE gene product of *Escherichia coli*. *J Bacteriol.* 1981; 145:513–520. [PubMed: 6161915]
37. McNulty BC, Young GB, Pielak GJ. Macromolecular crowding in the *Escherichia coli* periplasm maintains alpha-synuclein disorder. *J Mol Biol.* 2006; 355:893–897. [PubMed: 16343531]
38. Tapley TL, Franzmann TM, Chakraborty S, Jakob U, Bardwell JCA. Protein refolding by pH-triggered chaperone binding and release. *Proc Natl Acad Sci U S A.* 2010; 107:1071–1076. [PubMed: 20080625]
39. Miller, JH. *A Short Course in Bacterial Genetics.* CSHL Press; Plainview, NY: 1992. p. 135-142.
40. Hiniker A, Bardwell JCA. In vivo substrate specificity of periplasmic disulfide oxidoreductases. *J Biol Chem.* 2004; 279:12967–12973. [PubMed: 14726535]
41. Otwinowski Z, Minor W. Processing of X-ray diffraction data collected in oscillation mode. *Macromolecular Crystallography, Pt A.* 1997; 276:307–326.
42. Vonrhein C, Blanc E, Roversi P, Bricogne G. Automated structure solution with autoSHARP. *Methods Mol Biol.* 2007; 364:215–230. [PubMed: 17172768]
43. Emsley P, Cowtan K. Coot: model-building tools for molecular graphics. *Acta Crystallogr D Biol Crystallogr.* 2004; 60:2126–2132. [PubMed: 15572765]
44. Murshudov GN, Vagin AA, Dodson EJ. Refinement of macromolecular structures by the maximum-likelihood method. *Acta Crystallogr D Biol Crystallogr.* 1997; 53:240–255. [PubMed: 15299926]
45. Adams PD, et al. PHENIX: a comprehensive Python-based system for macromolecular structure solution. *Acta Crystallogr D Biol Crystallogr.* 2010; 66:213–221. [PubMed: 20124702]
46. Chen VB, et al. MolProbity: all-atom structure validation for macromolecular crystallography. *Acta Crystallogr D Biol Crystallogr.* 2010; 66:12–21. [PubMed: 20057044]
47. Hennecke J, Sebbel P, Glockshuber R. Random circular permutation of DsbA reveals segments that are essential for protein folding and stability. *J Mol Biol.* 1999; 286:1197–1215. [PubMed: 10047491]
48. Quan S, Schneider I, Pan J, Hacht AV, Bardwell JC. The CXXC motif is more than a redox rheostat. *J Biol Chem.* 2007; 282:28823–28833. [PubMed: 17675287]
49. Baba T, et al. Construction of *Escherichia coli* K-12 in-frame, single-gene knockout mutants: the Keio collection. *Mol Syst Biol.* 2006; 2:2006.0008.
50. Jonda S, Huber-Wunderlich M, Glockshuber R, Mossner E. Complementation of DsbA deficiency with secreted thioredoxin variants reveals the crucial role of an efficient dithiol oxidant for

- catalyzed protein folding in the bacterial periplasm. *EMBO J.* 1999; 18:3271–3281. [PubMed: 10369668]
51. Datsenko KA, Wanner BL. One-step inactivation of chromosomal genes in *Escherichia coli* K-12 using PCR products. *Proc Natl Acad Sci U S A.* 2000; 97:6640–6645. [PubMed: 10829079]
 52. Bochner BR, Huang HC, Schieven GL, Ames BN. Positive selection for loss of tetracycline resistance. *J Bacteriol.* 1980; 143:926–933. [PubMed: 6259126]
 53. Cherepanov PP, Wackernagel W. Gene disruption in *Escherichia coli*: TcR and KmR cassettes with the option of Flp-catalyzed excision of the antibiotic-resistance determinant. *Gene.* 1995; 158:9–14. [PubMed: 7789817]
 54. Chen Y, et al. Crystal structure of human histone lysine-specific demethylase 1 (LSD1). *Proc Natl Acad Sci U S A.* 2006; 103:13956–13961. [PubMed: 16956976]
 55. Hayer-Hartl M. Assay of malate dehydrogenase. A substrate for the *E. coli* chaperonins GroEL and GroES. *Methods Mol Biol.* 2000; 140:127–132. [PubMed: 11484479]
 56. Bader MW, Xie T, Yu CA, Bardwell JC. Disulfide bonds are generated by quinone reduction. *J Biol Chem.* 2000; 275:26082–26088. [PubMed: 10854438]
 57. Nijkamp HJJ, et al. The complete nucleotide-sequence of the bacteriocinogenic plasmid Clodf13. *Plasmid.* 1986; 16:135–160. [PubMed: 3749334]

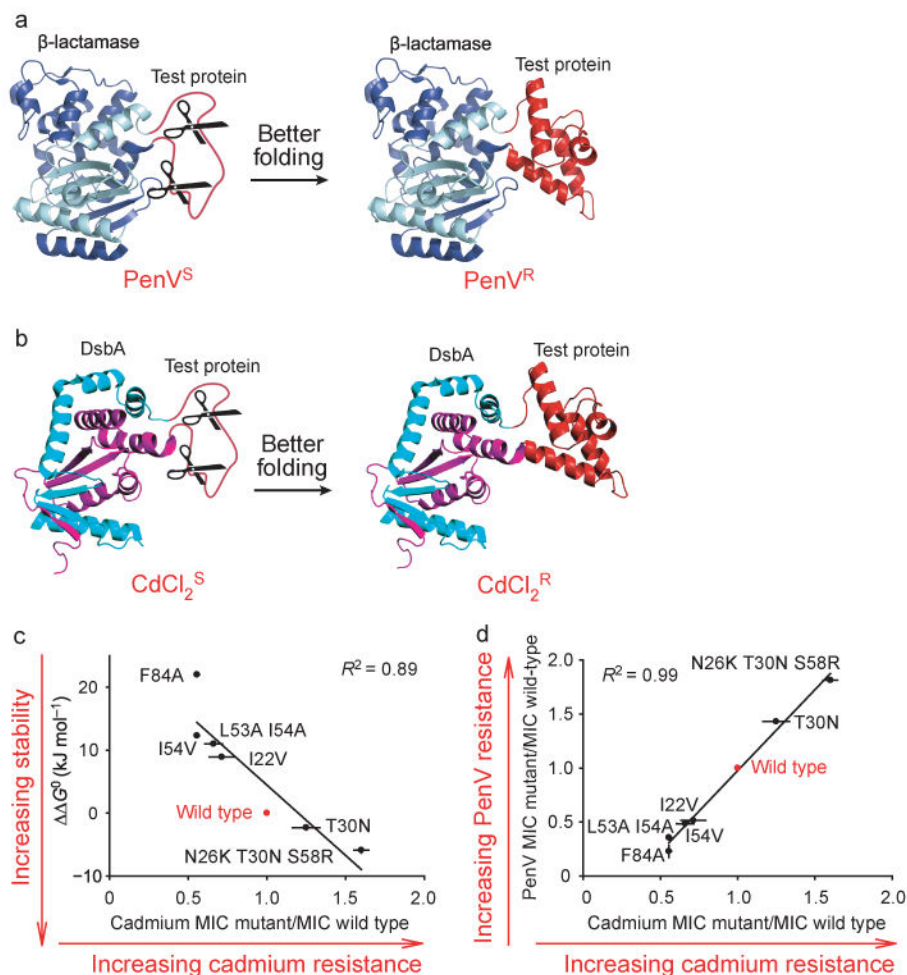


Figure 1. A dual fusion selection for enhancing *in vivo* protein stability. **(a)** Unstable test proteins inserted into β -lactamase are degraded by cellular proteases, producing penicillin sensitive (PenV^S) strains. Improving the folding of the test proteins increases penicillin resistance (PenV^R). **(b)** Insertion of unstable test proteins into DsbA renders the strains sensitive to cadmium (CdCl_2^S). Improving the folding of the test proteins increases the strains' resistance towards cadmium (CdCl_2^R). **(c)** Thermodynamic stability of Im7 variants (given as $\Delta\Delta G^0$ relative to wild-type Im7) correlates with the minimal inhibitory concentration (MIC) of cadmium for cells expressing the DsbA fusions to these variants. **(d)** Penicillin resistance of cells expressing the β -lactamase-Im7 fusions correlates with cadmium resistance when they also express the DsbA-Im7 fusion proteins with the same Im7 variants. Error bars indicate the s.d. of three independent measurements.

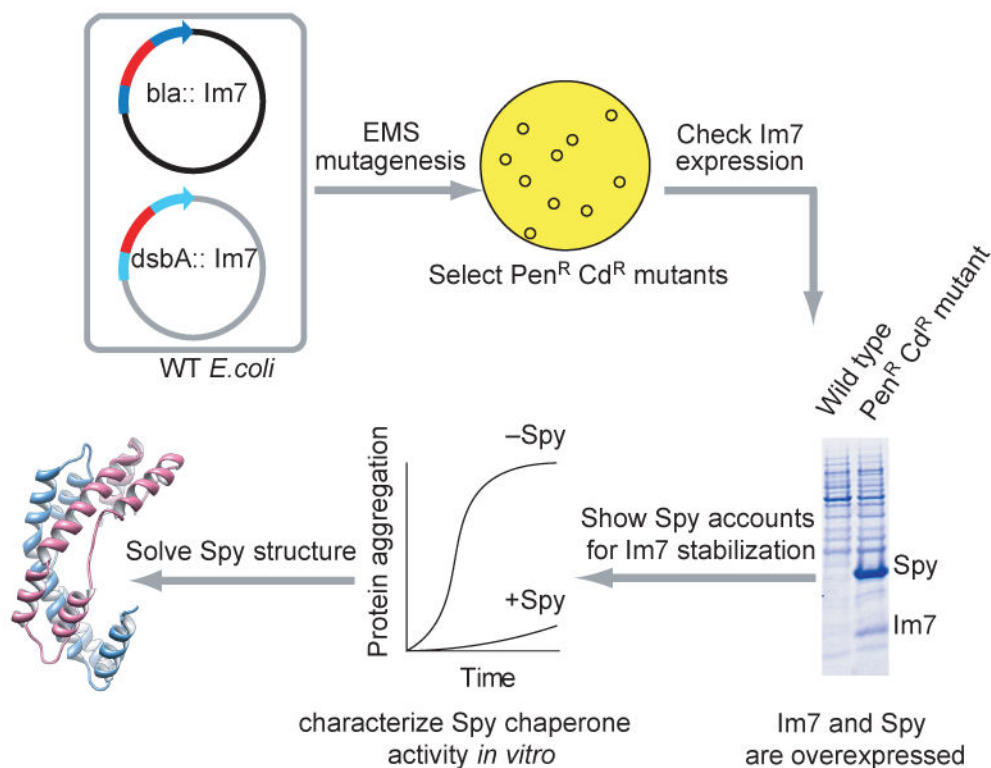


Figure 2. Overall experimental scheme. Fusion constructs that link the stability of the poorly folded Im7 protein to Pen^V^R (*bla::Im7*) and to CdCl₂^R (*dsbA::Im7*) were introduced into the same *E. coli* strain. Following mutagenesis by EMS treatment, mutants that simultaneously enhanced both Pen^V^R and CdCl₂^R were selected, and levels of Im7 in these strains were measured. The mutants massively increased levels of Im7 as well as a host protein called Spy. Genetic experiments showed that increased Spy levels are necessary and sufficient to increase Im7 levels. The Spy protein was examined for molecular chaperone activity *in vitro* and was found to be highly effective as a chaperone in preventing protein aggregation and aiding refolding. Spy was then crystallized, its structure was solved and mutants were made based on its structure to explore the interaction of Spy with its substrates.

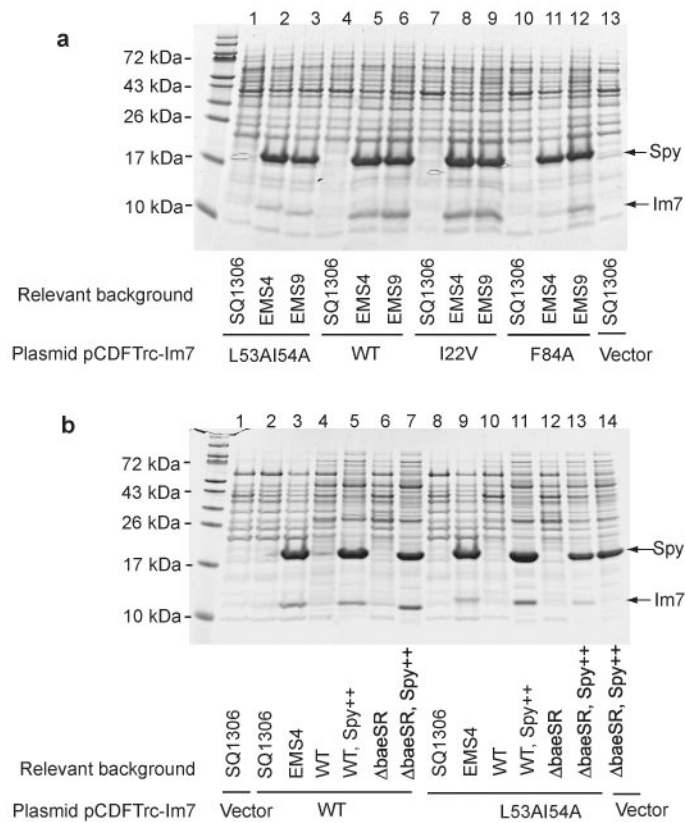


Figure 3. Im7 and Spy are abundant in the periplasm of EMS strains. **(a)** The PenV^R and CdCl₂^R resistant mutants EMS4 and EMS9 and the parental SQ1306 strain were transformed with plasmids encoding wild-type Im7 (WT) or the destabilized variants L53A I54A, I22V, and F84A3, 6. Periplasmic extracts were prepared and analyzed by SDS-PAGE. **(b)** Spy overexpression is sufficient to enhance Im7 levels in both wild-type and *baeSR* backgrounds to those seen in EMS4. Plasmid-encoded Im7 and its destabilized variants were expressed in SQ765 wild-type (WT) or *baeSR* backgrounds, with or without the co-expression of plasmid-encoded Spy (designated as Spy⁺⁺). Aggregated or insoluble Spy is not expected to be extracted using our periplasmic extraction procedure and therefore will not be detected in these experiments.

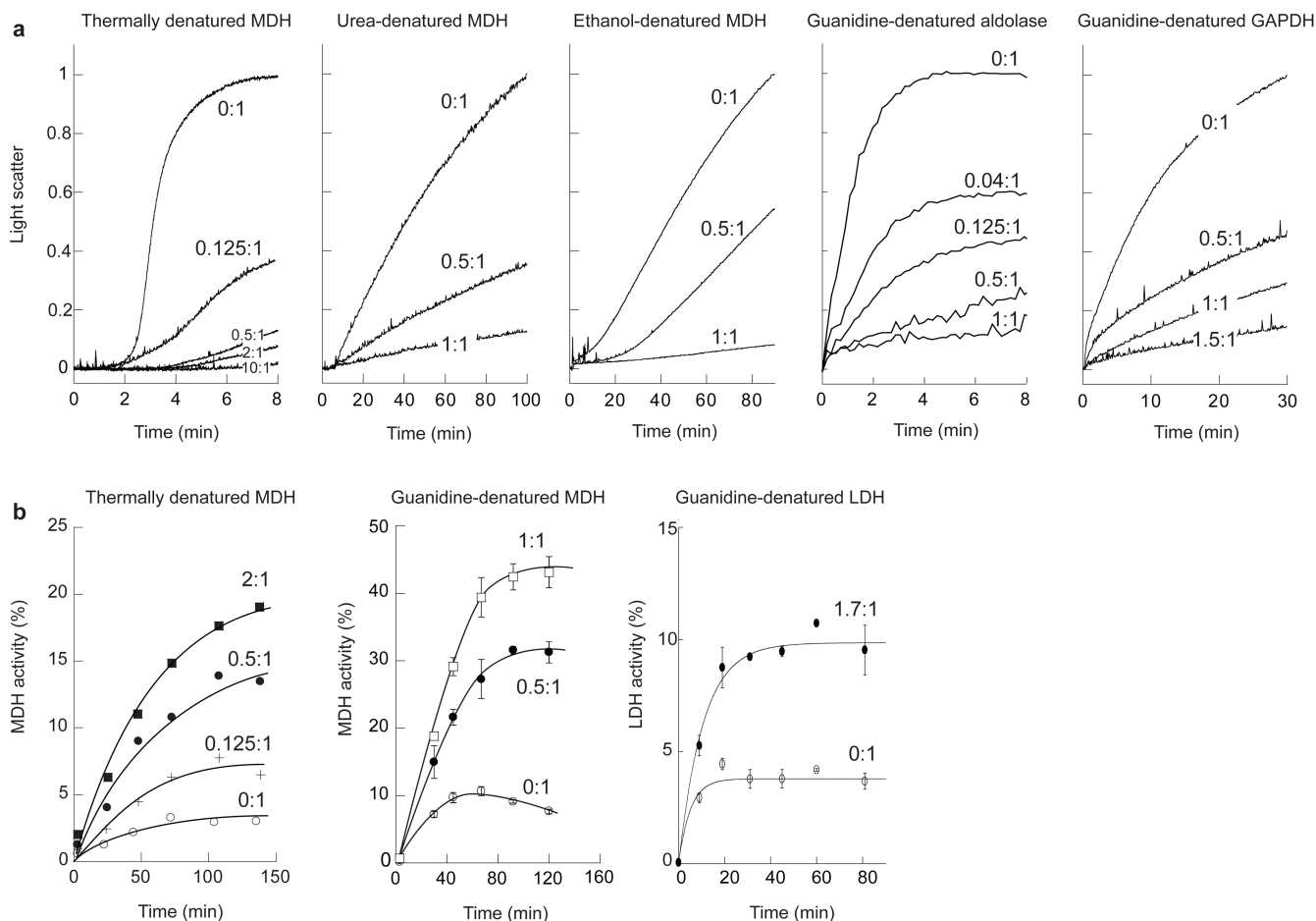


Figure 4. Spy has chaperone activity. **(a)** Spy suppresses protein aggregation as monitored by light scattering. Aggregate formation in the absence (0:1) and presence of increasing amounts of Spy (ratios given are Spy:substrate) was monitored for thermally (43 °C) or chemically denatured substrates. **(b)** Spy enhances protein refolding as assessed by recovery of enzymatic activity. Refolding was monitored in the absence (0:1) and presence of Spy for thermally (43 °C) or chemically denatured substrates. Plots show mean \pm s.d. of three independent measurements. Ultracentrifugation and gel filtration studies (Supplementary Fig. 6) indicate that Spy is dimeric in solution, so Spy concentrations are given as a dimer.

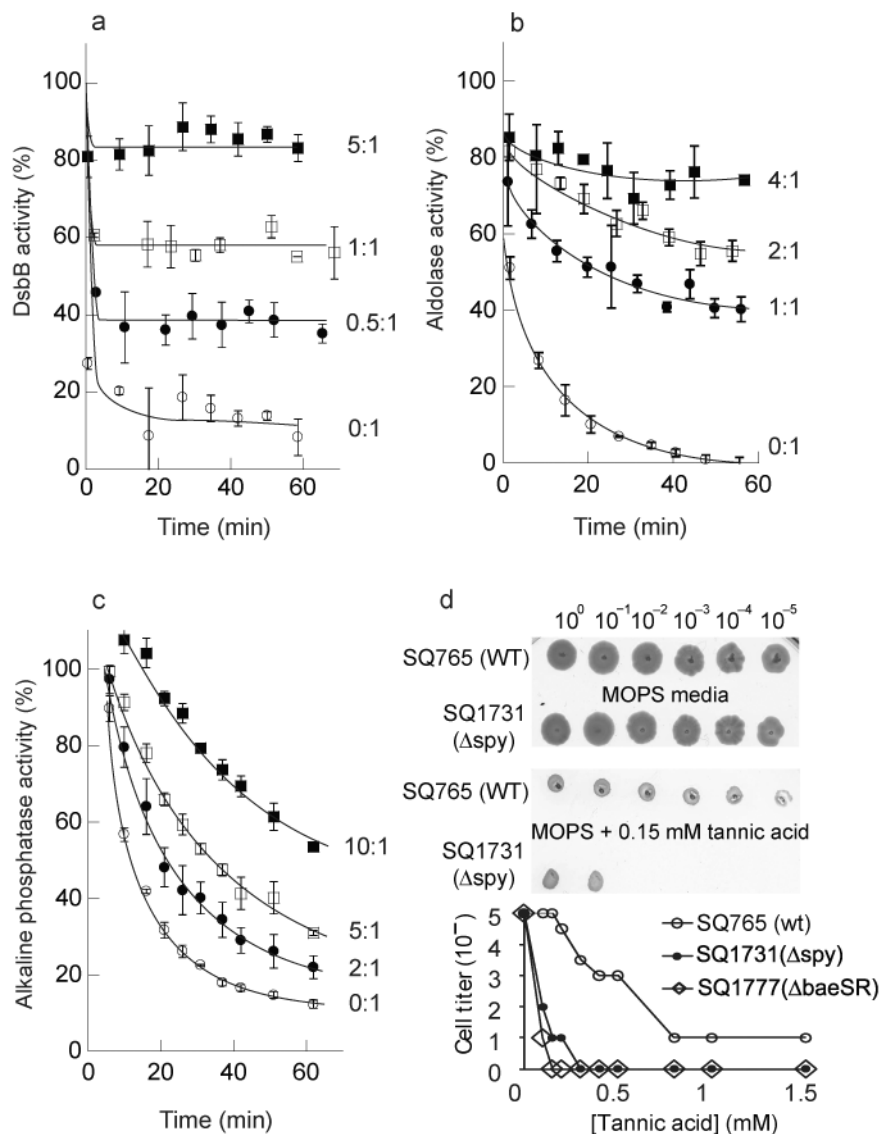


Figure 5. Spy protects DsbB, aldolase, and alkaline phosphatase from tannic acid-induced activity loss. Spy concentrations are given as a dimer. Plots show mean \pm s.d. for three independent measurements. **(a)** Enzymatic activity of *E. coli* DsbB (0.5 μ M) incubated in 100 μ M tannic acid in the absence (0:1) or presence of increasing amounts of Spy (ratios given are Spy:substrate). **(b)** Enzymatic activity of rabbit muscle aldolase (0.5 μ M) incubated in 16 μ M tannic acid in the absence or presence of increasing amounts of Spy. **(c)** Enzymatic activity of *E. coli* alkaline phosphatase (AP) (1 μ M) incubated in 500 μ M tannic acid in the absence or presence of increasing amounts of Spy. **(d)** Spy and BaeSR deletion strains are tannin sensitive.

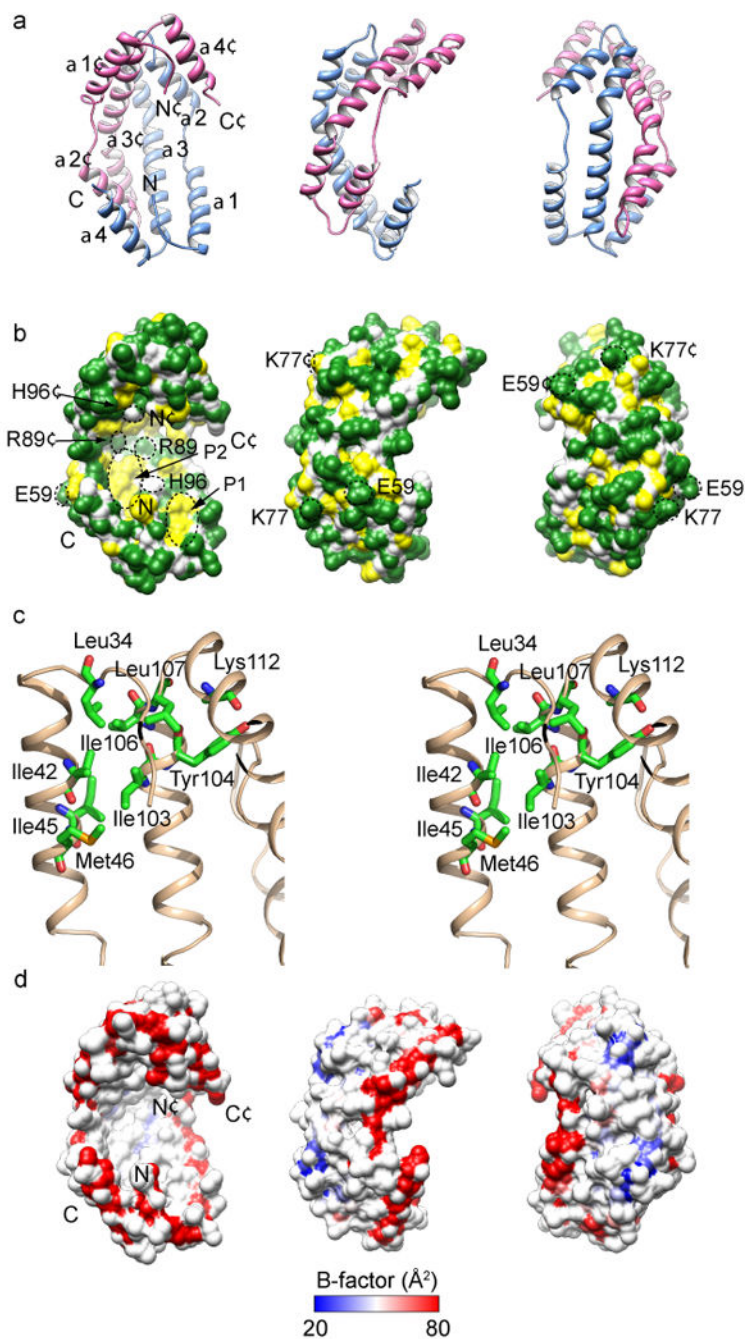


Figure 6. Crystal structure of the Spy dimer shown in three orientations rotated by 90° along the vertical axis. For ease of comparison the orientations shown in parts a, b, d are identical. (a) Ribbon drawing shows an all α -helical structure. One subunit is colored light blue and the other is colored magenta. The N and C termini and the secondary structural elements of the molecule are labeled. (b) Surface properties of Spy, colored based on the underlying atoms: backbone atoms, white; polar and charged side-chain atoms, green; hydrophobic side-chain atoms, yellow. Two predominantly hydrophobic patches in the concave surface are indicated

as P1 and P2. The lower right patch (P1) is composed of Leu34, Ile42, Met46 and Ile103. The upper left patch (P2) is composed of Pro56, Met64, Ile68, Met85, Met93 and Met97. The residues labeled with fluorescent probes (for experiments in Fig. 7) are circled in black. (c) Stereoview showing the cluster of hydrophobic residues at the tip of the cradle marked as P1 in panel (b). (d) Structural flexibility of Spy dimer. The molecular surface representing the Spy backbone atoms is colored based on the average backbone B-factors for each residue. Note that the rim lining the concave surface has higher B-factors, indicating greater structural flexibility. In particular, the N and C termini are highly mobile. These residues are well conserved among homologous sequences (Supplementary Fig. 5).

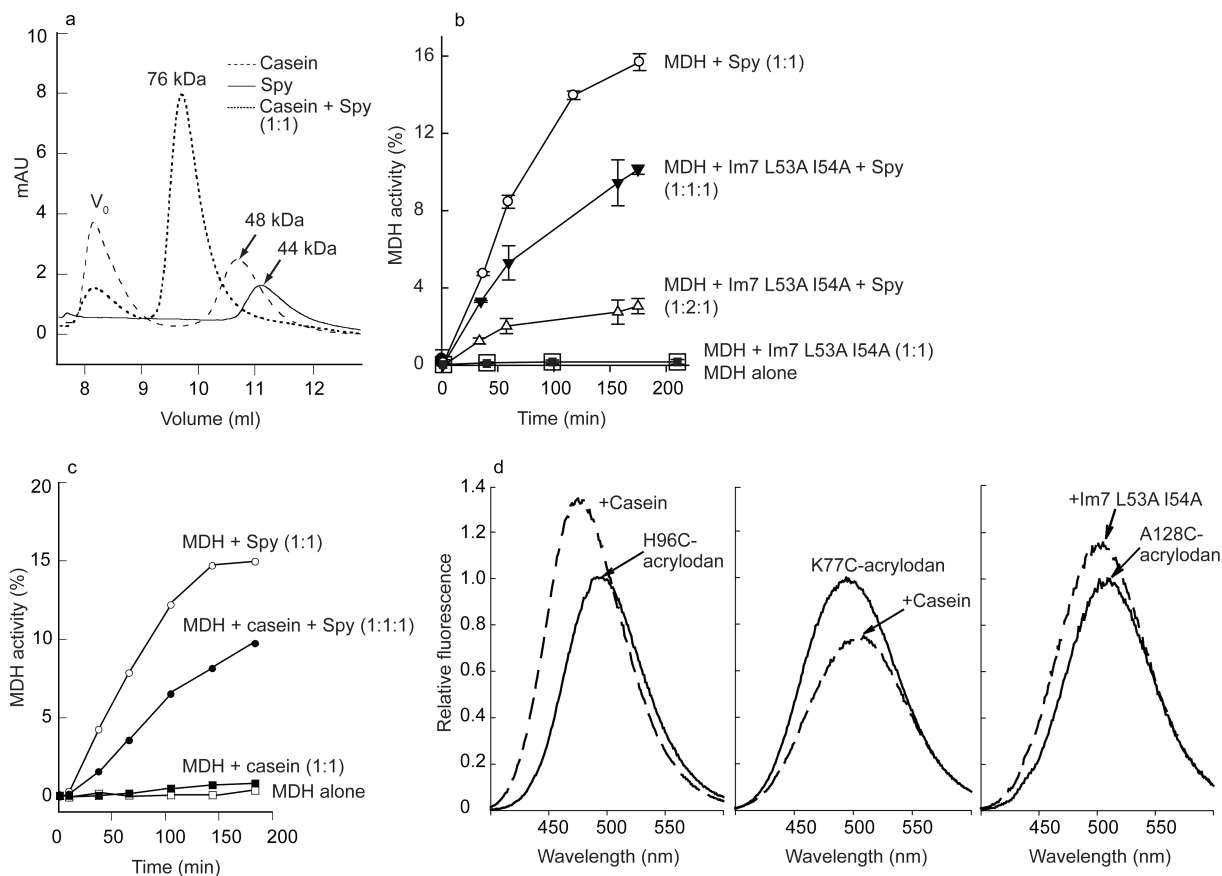


Figure 7. Spy binds the disordered model substrate protein casein and the *in vivo* substrate protein Im7-L53A I54A. (a) Analytical gel filtration of Spy alone, casein alone, or a 1:1 mixture of Spy and casein. The molecular weight of a dimer of Spy is 31 kDa, but it elutes as a 44 kDa molecule, which is consistent with the elongated form of the dimer as seen in the crystal structure. The molecular weight of casein is 23–26 kDa. (b) Competition assay between urea-denatured Im7-L53A I54A and MDH for Spy in MDH refolding. Refolding of chemically denatured MDH was monitored by recovery of enzymatic activity plotted as a fraction of the activity of native (*i.e.*, nondenatured) MDH. Note that the curves of MDH alone (open squares) and MDH + Im7-L53A I54A (closed squares) overlap precisely. (c) Competition assay between casein and MDH for Spy binding. Refolding of chemically denatured MDH was monitored as in (b). (d) Normalized fluorescence emission spectra of acrylodan-labeled Spy mutants H96C and K77C in the absence or presence of an equimolar amount of casein. Note that the fluorescence change upon casein addition for Spy K77-acrylodan is opposite that from Spy H96C-acrylodan. (e) Normalized fluorescence emission spectra of acrylodan-labeled Spy A128C in the absence or presence of an equimolar amount of urea-denatured Im7-L53A I54A.

Table 1
Spy induction increases Im7 levels substantially

Strains compared	Relevant host genotypes* compared	Im7 variant	Fold increase in Im7 level
SQ1406/SQ1414	EMS4/WT	L53A I54A	66 ± 28
SQ1410/SQ1414	EMS9/WT	L53A I54A	92 ± 44
SQ1805/SQ1809	<i>spy</i> ⁺⁺ /WT	L53A I54A	280 ± 145
SQ1826/SQ1830	<i>baeSR, spy</i> ⁺⁺ / <i>baeSR</i>	L53A I54A	684 ± 162
SQ1405/SQ1413	EMS4/WT	WT	34 ± 12
SQ1409/SQ1413	EMS9/WT	WT	43 ± 24
SQ1804/SQ1808	<i>spy</i> ⁺⁺ /WT	WT	165 ± 93
SQ1825/SQ1829	<i>baeSR, spy</i> ⁺⁺ / <i>baeSR</i>	WT	211 ± 83
SQ1407/SQ1415	EMS4/WT	I22V	51 ± 9
SQ1411/SQ1415	EMS9/WT	I22V	48 ± 23
SQ1806/SQ1810	<i>spy</i> ⁺⁺ /WT	I22V	103 ± 14
SQ1827/SQ1831	<i>baeSR, spy</i> ⁺⁺ / <i>baeSR</i>	I22V	470 ± 176
SQ1408/SQ1416	EMS4/WT	F84A	43 ± 18
SQ1412/SQ1416	EMS9/WT	F84A	67 ± 16
SQ1807/SQ1811	<i>spy</i> ⁺⁺ /WT	F84A	694 ± 243
SQ1828/SQ1832	<i>baeSR, spy</i> ⁺⁺ / <i>baeSR</i>	F84A	589 ± 102

Data indicate extent of Im7 overproduction in various strains (see Supplementary Table 1a for details of strains). Fold increases in Im7 levels were quantified with an Agilent Bioanalyzer 2100 by direct comparison between periplasmic extracts prepared from various pairs of strains (see Methods). Values are the average of measurements from three biological samples ± s.d.. WT, wild type.

* *spy*⁺⁺ designates cells that overexpress Spy from pTrc-spy.

Table 2
Data collection, phasing and refinement statistics for Spy

SeMet Data	
Data collection	
Space group	P6 ₂
Cell dimensions	
<i>a</i> , <i>b</i> , <i>c</i> (Å)	69.0, 69.0, 124.3
<i>α</i> , <i>β</i> , <i>γ</i> (°)	90, 90, 120
Wavelength	0.9792
Resolution (Å) *	50-2.6 (2.66-2.6)
<i>R</i> _{sym} or <i>R</i> _{merge} *	0.116 (0.575)
<i>I</i> / <i>σI</i> *	37.1 (2.9)
Completeness (%) *	97.8 (83.1)
Redundancy *	9.3 (5.2)
Refinement	
Resolution (Å)	2.6
No. reflections	10139
<i>R</i> _{work} / <i>R</i> _{free}	0.243/0.281
No. atoms	
Protein	1512
Ion	21
Water	9
<i>B</i> -factors	
Protein	81
Ion	63
Water	83
R.m.s deviations	
Bond lengths (Å)	0.014
Bond angles (°)	1.32

* Values in parenthesis correspond to the highest resolution outer shell.

There are two independent molecules in the asymmetric unit, each containing 11 Met residues. The molecules are related by a non-crystallographic 2-fold symmetry and are very similar. No NCS restraints were applied during refinement and the two molecules superimpose with rmsd of 0.3 Å for 96 C-alpha atoms and 1.1 Å for all atoms.